Transmission of TE-polarized light through metallic nanoslit arrays assisted by a quasi surface wave

2014 Appl. Phys. Express 7 032001

(http://iopscience.iop.org/1882-0786/7/3/032001)

Applied Physics Express 7, 032001 (2014)
http://dx.doi.org/10.7567/APEX.7.032001

Transmission of TE-polarized light through metallic nanoslit arrays assisted by a quasi surface wave

Zhijun Sun*, Tengpeng Guan, Wei Chen, and Xiaoliu Zuo

Department of Physics, Xiamen University, Xiamen 361005, China
E-mail: sunzj@xmu.edu.cn

Received November 4, 2013; accepted January 21, 2014; published online February 6, 2014

Optically thick metallic nanoslit arrays are opaque to TE-polarized light, in contrast to enhanced transmission of TM-polarized light. Here, we numerically show that, by introducing an ultrathin high-index dielectric coating on the metal surfaces, a quasi surface wave can be excited at the metasurfaces to enhance the transmission of TE-polarized light. The quasi surface wave is shown to behave like surface plasmon waves, and enhance the transmission in similar mechanisms as surface plasmon waves do for TM-polarized light. In this work, we suggest a way of manipulating TE-polarized light in metallic subwavelength structures. © 2014 The Japan Society of Applied Physics

It is known that the transmission of light through nanoapertured thick metal films is due to the excitation of surface plasmons (SPs), which carry the coupled optical energy to propagate and oscillate in the nanoscale, resulting in enhanced transmission.[1–7] However, SPs can be excited at metal surfaces with only transverse-magnetically (TM) polarized light;[8] thus, the transverse-electrically (TE) polarized component of the light is usually excluded from mesoscopic optical interactions in metallic nanostructures. For example, metallic nanoslit arrays, to which purely TE or TM polarization states of incidence light can be defined, allow transmission of TM-polarized light but not the TE-polarized one. It was reported in a few studies that dielectrics can be introduced in apertured metallic structures for transmission of *s*-polarized light (i.e., TE-polarized here).[9–11] However, in those works, the metal layers are rather thin, and the slits are wide relative to the wavelength of the light and are fully filled with the dielectric media besides a thick coating of the dielectric; these conditions allow conventional waveguiding modes in the slits for transmission of TE-polarized light.

In this work, we show that, by introducing an ultrathin high-index dielectric (HID) coating on the metallic nanoslit structures, prominent transmission of TE-polarized light is achieved owing to the excitation of a quasi surface wave, in parallel with that of SP-enhanced transmission of TM-polarized light. Compared with the findings described in Refs. 9–11, our approach allows transmission through rather narrow slits perforated in thick metal films, and the empty slits provide versatility in applications of this structure. Besides, the characteristics and mechanisms of the enhanced transmission are different arising from the role of the quasi surface waves. Figure 1(a) is a schematic illustration of the HID-coated silver metallic nanoslit array on a transparent quartz substrate. The HID layer may be coated using an isotropic film deposition process (e.g., chemical vapor deposition) after the fabrication of the metallic nanostructure. Moreover, a high index of the coating layer may be found in some semiconductors (e.g., amorphous silicon) for operations in the visible-to-near-infrared (VIS–NIR) range, as will be seen later.

In Fig. 1(b), we show transmission spectra of the modified metallic nanoslit arrays under normal incidence of TE-polarized light. The results are obtained from numerical simulations based on the finite-difference time-domain (FDTD) method. Here, we assume that the HID layer of index $n_c = 4$ and thickness $t_c = 20\,\text{nm}$ is uniformly coated on the metallic nanoslit arrays with a period $p = 400\,\text{nm}$ and thickness $t = 150\,\text{nm}$, which results in a width of the slits $s = 60\,\text{nm}$. The index of the substrate is taken to be 1.45 for quartz. It is observed that a high transmission of the TE-polarized light appears in particular bands, in contrast to the extremely low transmission continuum of the one without any coating of the HID layer; meanwhile, a clear null transmission dip appears at $\lambda_0 = 512\,\text{nm}$, similar to that due to in-plane SP resonance at the surface of metallic nanoslit arrays for the transmission of TM-polarized light.[4–7,12] Transmission spectra for TM-polarized light in Fig. 1(c) are plotted for reference. As expected, high transmission bands are demonstrated for both cases; addition of the HID coating results in a large redshift of the main transmission peak. In Fig. 1(d), TE-polarization transmission spectra of the structures with the HID coatings partially removed are calculated to observe the effects of individual segments of the HID layers on transmission. Observations reveal that HID layers at the sidewalls of the slits are critical for a high transmission, while the top HID layers define the null-transmission dips. Moreover, the HID layer at the bottom of the slits can be removed, which also allows the transmission of TE-polarized light except for a blue-shift of the main transmission peak owing to a reduction of the general effective index in the slits. In the following, we analyze the transmission mechanisms with emphasis on the role of the HID layers.

Firstly, we show how coating of the HID layer can enable the metallic nanostructures to interact with TE-polarized light. Optical waves are usually subject to the diffraction limit. To squeeze a propagating wave into a deep-subwavelength scale, a surface mode with transverse evanescent distribution of the field is usually essential, e.g., the SP waves. However, for ordinary dielectric and metallic materials, no TE-polarized surface mode exists at their interfaces, restricted by boundary conditions. It is known that, when a dielectric layer is deposited on a metal surface forming a metal–dielectric–air (MDA) structure, TE waveguide modes can exist in the dielectric layer.[13] Usually, as the index of the dielectric layer is relatively low, the cut-off thickness of the dielectric layer is in an order of half-wavelength, as illustrated in Fig. 2(a). However, if the dielectric layer has a high index, the thickness of the dielectric layer can be largely reduced to a nanoscale. Thus, the TE waveguide mode will have a quasi-evanescent transverse distribution of the transverse electric field (E_y), as shown in Fig. 2(b) for the MDA structure. It is like that of a surface wave, e.g., the distribution

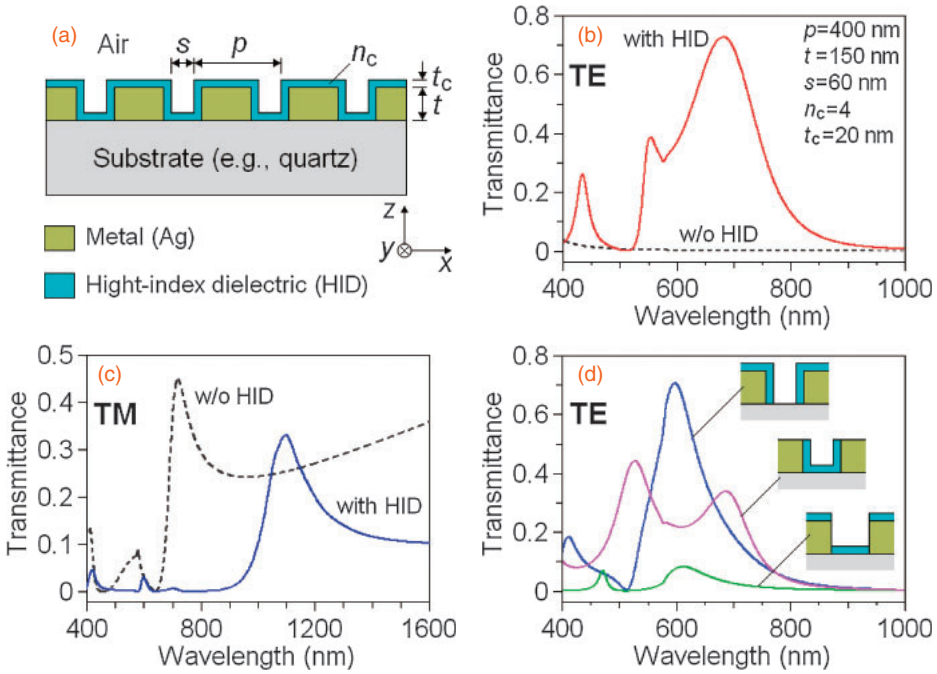

Fig. 1. (a) Schematic illustration of metallic nanoslit array coated with an HID layer. (b, c) Transmission spectra of an HID-modified structure for TE- and TM-polarized light (for reference), in comparison with those of structures without any HID coating. (d) TE transmission spectra of the structure in (b) with its HID layers partially removed.

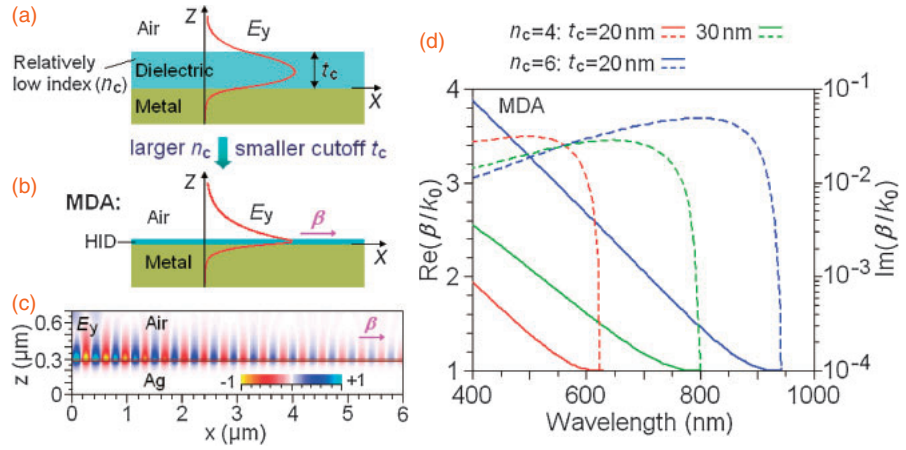

Fig. 2. (a) Schematic field distribution of fundamental TE waveguide mode in a thick low-index dielectric layer on a metal surface. (b) Quasi-evanescent distributions of the field for TE-mode quasi surface waves at an ultrathin HID-modified MDA surface, analytically calculated for $n_c = 4$, $t_c = 20$ nm at $\lambda_0 = 500$ nm. (c) Simulation of the propagating wave in (b). (d) Normalized real (solid line) and imaginary (dashed line) propagation constants of quasi surface waves at different MDA surfaces.

of the transverse magnetic field (H_y) of a TM-polarized SP wave mode. As such, we consider it as a quasi surface wave, locating at an HID-coated metasurface of metal. In Fig. 2(c), propagation of the quasi surface wave at the MDA metasurface is simulated, mimicking that of SP waves. In Fig. 2(d), the normalized complex propagation constant (β/k_0, $k_0 = 2\pi/\lambda_0$) or effective index ($N_{\text{eff}} = \beta/k_0$) of the TE-mode quasi surface wave is plotted as a function of the wavelength for HID layers of $n_c = 4$ and 6 and $t_c = 20$ and 30 nm. For a given set of the HID parameters, the cut-off wavelength is clearly indicated, e.g., at $\lambda_0 = 630$ nm for $n_c = 4$ and $t_c = 20$ nm. Thus, the quasi surface wave exists only below the cut-off wavelength, beyond which the field cannot be effectively confined near the metal surface. The results suggest that a medium of higher index is preferred for the HID layer, which allows a thinner HID layer and the existence of the quasi surface wave in a wider VIS–NIR spectrum range.

Moreover, the ultrasmall thickness of the dielectric layer allows its incorporation into subwavelength metal structures. For instance, a metallic subwavelength gap can be so modified to form the metal–dielectric–air–dielectric–metal (MDADM) gap structure shown in Fig. 3(a), whose fundamental TE mode also has a field distribution similar to that of an SP gap mode.[13,14] This indicates the possibility of squeezing the TE-polarized light into metallic nanostructures for mesoscopic interactions. In Fig. 3(c), dependences of the normalized propagation constant on wavelength are shown for the guiding mode in an MDADM gap with HID layers of

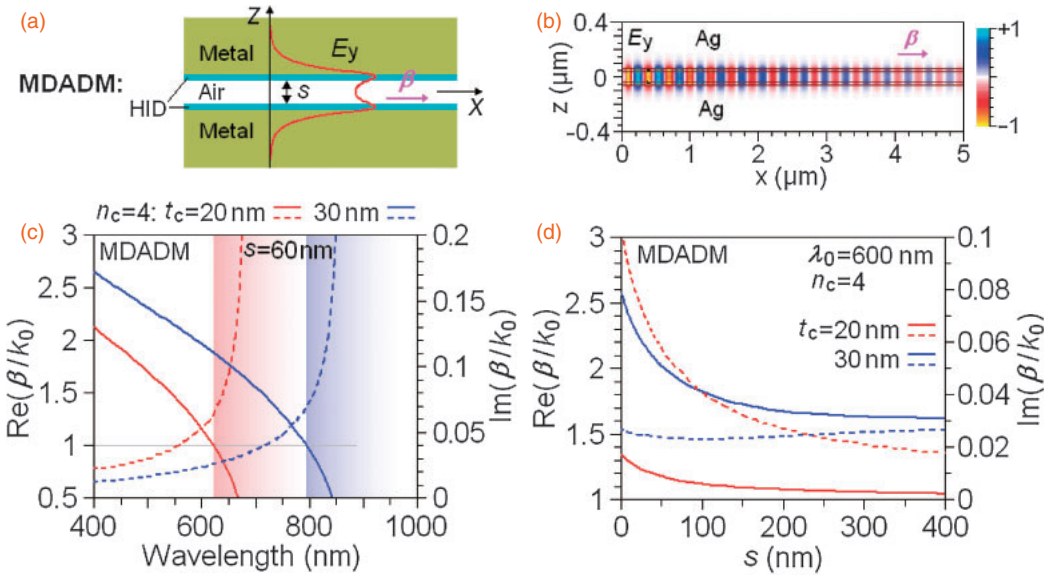

Fig. 3. (a) Transverse distributions of the field for TE-mode quasi surface waves in an MDADM gap waveguide, analytically calculated for $n_c = 4$, $t_c = 20\,\text{nm}$, and $s = 80\,\text{nm}$ at $\lambda_0 = 500\,\text{nm}$. (c) Simulated field of the propagating wave in (a). (c) Normalized real (solid line) and imaginary (dash line) propagation constants of quasi surface waves in MDADM gap waveguides and their dependences on gap width at $\lambda_0 = 600\,\text{nm}$ (d).

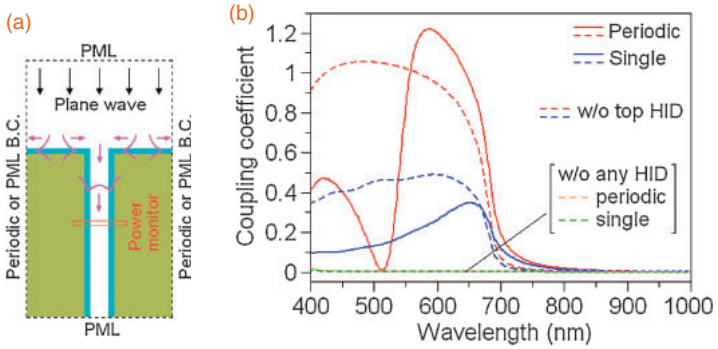

Fig. 4. Coupling of TE-polarized light into an HID-modified metallic nanoslit. (a) Schematic model in simulation analysis. (b) Coupling coefficient as a function of wavelength for the slit ($n_c = 4$, $t_c = 20\,\text{nm}$, $s = 60\,\text{nm}$) being in a period array ($p = 400\,\text{nm}$) or single, and those when the top or all parts of the HID layers are removed.

$n_c = 4$, $t_c = 20$ or $30\,\text{nm}$, and a slit width of $s = 60\,\text{nm}$. Unlike the mode at an MDA surface, a cut-off wavelength is defined here corresponding to $\text{Re}(\beta/k_0) = 1$ for the MDADM gap mode. When $\text{Re}(\beta/k_0) < 1$ [shaded regimes in Fig. 3(c)], it becomes a leaky mode; the power is strongly attenuated as if propagating in a bulk metal. In Fig. 3(d), dependences of the normalized propagation constant on gap width are shown for the MDADM waveguides of $n_c = 4$ and $t_c = 20$ or $30\,\text{nm}$ at $\lambda_0 = 600\,\text{nm}$. These results show that the characteristics of the quasi surface wave mode at an MDA metasurface or in an MDADM gap are qualitatively similar to those of the SP modes in general. As for the existence of the cut-off, it exists also for the SP waves in fact — as we know, there are no SP waves in the long-wavelength range where noble metals are perfect conductors. That is how the terminology of "spoof surface plasmons" is used for the SP-like waves in microwave and terahertz regimes.[15,16] Simply, the SP waves intrinsically exist in a relatively broad band.

Next, we study the coupling of TE-polarized light into an HID-modified metallic nanoslit, as illustrated in Fig. 4(a), by FDTD simulations. To exclude the effects of cavity resonances in the slit, the slit is assumed to have a semi-infinite length. As neighboring slits may optically interact, we treated two cases of the slit being either in a periodic array or just a single one to see the effect of periodicity. For them, the periodic or perfect matching layer (PML) boundary conditions (BCs) are applied in lateral directions of the simulation region. Note that, under periodic BC, the width of the simulation region is the period; however, under the PML BC for a single slit, the simulation region width is set to be large enough so that the power "funneled" into the slit from the top surface can all be counted. Here, a coupling coefficient is defined for evaluation as the ratio of the power coupled into the slit to the power of the incident plane wave light within a width corresponding to the metal slit ($s + 2t_c$). Figure 4(b) shows the calculated coupling coefficients as functions of wavelength, together with those of cases without the top only or all parts of the HID layers ($n_c = 4$, $t_c = 20\,\text{nm}$, $s = 60\,\text{nm}$). It is clearly demonstrated that, without the HID layers, there is almost no power coupled into the slit whether it is single or in a periodic array. Beyond the cut-off wavelength of the gap surface wave mode ($\sim\lambda_0 = 650\,\text{nm}$), the

coupling coefficients decrease sharply to near zero for all cases of the HID-modified slits. It is found that, for the slit in a periodic array ($p = 400$ nm), there is a distinct dip of the coupling coefficient at $\lambda_0 = 512$ nm, corresponding to in-plane resonances of the quasi surface waves at the top MDA metasurface, as also shown in the transmission spectra in Fig. 1(b). Otherwise, the slit in a periodic array has a much higher coupling coefficient than the single slit in general; moreover, at its maximum (at around $\lambda_0 = 587$ nm), the coefficient is even larger than one. We think that the presence of the slits in periodicity prohibits long propagation of the nonresonant quasi surface waves at the top MDA surface, which renders more flow of the surface wave power into the slits, resulting in a larger coupling coefficient. It is also observed that, for the slit in a periodic array, removal of the top surface HID layer results in the disappearance of the dip, as the corresponding in-plane resonance mode is not supported without the HID layer. However, in the single-slit case, when the top HID layer is removed, the coupling coefficient is enhanced below the cut-off. This is thought to be attributable to the reduction of other channels (coupling into the surface mode at the top surface) upon scattering of incident light at the slit entrance.

The analyses above show that modification of metallic nanoslit arrays with an HID coating layer provides a basis for the transmission of TE-polarized light via excitation of the quasi surface waves. However, the transmission is also subject to resonances in the metallic nanostructures, which can be considered in reference to the SP-enhanced transmission of TM-polarized light. In-plane resonance of the quasi surface wave at the periodically structured top MDA surface has been mentioned above, corresponding to the transmission dip at $\lambda_0 = 512$ nm in Fig. 1(b). This is further verified with the field distributions in Fig. 5(a), in which the resonant quasi surface wave locates at the top MDA surface like standing waves, and there is nearly no transmission of light. Positions of the in-plane resonance modes can usually be estimated with the equation: $\lambda_0^{\mathrm{res}} \approx N_{\mathrm{eff}}(\lambda_0^{\mathrm{res}}) \cdot p/m$, where λ_0^{res} is the resonance wavelength, N_{eff} is the effective index of the quasi surface wave, p is the period, and m is the resonance order. It is verified that, as $p = 400$ nm and $m = 1$, the above equation is satisfied at $\lambda_0 = 519$ nm for $N_{\mathrm{eff}} = 1.297$, close to the position of the transmission dip. Note that the deviation is due to the neglect of the Bloch-mode nature of the in-plane resonances, in which the transmission dip corresponds to a forbidden band gap instead of a specific wavelength.[12,17,18] Additionally, resonances in the slit cavities are also identified, which result in the transmission peaks at $\lambda_0 = 435$, 554, and 682 nm in Fig. 1(b). From field distributions at the peak positions in Figs. 5(b)–5(d), 2, 1, and 0 near-zero-field nodes are observed in the slits, corresponding to the 3rd-, 2nd-, and 1st-order resonances in the slit cavities, respectively.

From all the analyses above, it can be seen that, once the quasi surface wave mode is established by modification of the metallic nanostructures with an HID coating layer, the processes and mechanisms of transmission for TE-polarized light are similar to those of SP-assisted transmission for TM-polarized light.[3,12,19] Here, three coupled processes play critical roles in transmission under assistance of the quasi surface waves, i.e., funneled coupling of incident light into the slits, Bloch-mode resonances of the quasi surface waves at the top MDA surface, and cavity resonances in the slits. Besides, the effects of the quasi surface waves' cut-off in slits define the low transmission in the long-wavelength regime.

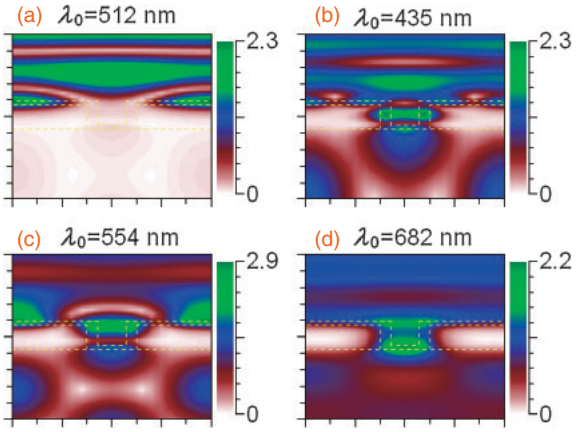

Fig. 5. Steady-state distributions of the field ($|E_y|$) within a period of the slit array at resonance positions in the transmission spectrum of Fig. 1(b). The light is normally incident from the top (air) side in the images.

In summary, a method is proposed to enable the transmission of TE-polarized light through metallic nanoslit arrays. The concept of quasi surface waves in an MDA metasurface also provides opportunities for the manipulation of TE-polarized light in metallic subwavelength structures or nanostructures, which can be used to devise novel micro/nanophotonics elements.

Acknowledgments The authors acknowledge the financial support from NSFC (No. 61275063), the Natural Science Foundation of Fujian Province of China (No. 2011J06002), and the Fundamental Research Funds for the Central Universities (No. 2012121009).

1) T. W. Ebbesen, H. J. Lezec, H. F. Ghaemi, T. Thio, and P. A. Wolff, Nature **391**, 667 (1998).
2) U. Schröter and D. Heitmann, Phys. Rev. B **58**, 15419 (1998).
3) J. A. Porto, F. J. García-Vidal, and J. B. Pendry, Phys. Rev. Lett. **83**, 2845 (1999).
4) L. Martín-Moreno, F. J. García-Vidal, H. J. Lezec, K. M. Pellerin, T. Thio, J. B. Pendry, and T. W. Ebbesen, Phys. Rev. Lett. **86**, 1114 (2001).
5) Z. Sun, Y. S. Jung, and H. K. Kim, Appl. Phys. Lett. **83**, 3021 (2003).
6) H. Liu and P. Lalanne, Nature **452**, 728 (2008).
7) F. J. Garcia-Vidal, L. Martin-Moreno, T. W. Ebbesen, and L. Kuipers, Rev. Mod. Phys. **82**, 729 (2010).
8) H. Raether, *Surface Plasmons on Smooth and Rough Surfaces and on Gratings* (Springer, Berlin, 1988).
9) E. Moreno, L. Martín-Moreno, and F. J. García-Vidal, J. Opt. A **8**, S94 (2006).
10) M. Guillaumée, A. Yu. Nikitin, M. J. K. Klein, L. A. Dunbar, V. Spassov, R. Eckert, L. Martín-Moreno, F. J. García-Vidal, and R. P. Stanley, Opt. Express **18**, 9722 (2010).
11) I. Schwarz, N. Livneh, and R. Rapaport, Opt. Express **20**, 426 (2012).
12) Z. Sun and D. Zeng, J. Mod. Opt. **55**, 1639 (2008).
13) I. P. Kaminow, W. L. Mammel, and H. P. Weber, Appl. Opt. **13**, 396 (1974).
14) L. Liu, Z. Han, and S. He, Opt. Express **13**, 6645 (2005).
15) J. B. Pendry, L. Martín-Moreno, and F. J. García-Vidal, Science **305**, 847 (2004).
16) N. Yu, Q. J. Wang, M. A. Kats, J. A. Fan, S. P. Khanna, L. Li, A. G. Davies, E. H. Linfield, and F. Capasso, Nat. Mater. **9**, 730 (2010).
17) Y. J. Chen, E. S. Koteles, R. J. Seymour, G. J. Sonek, and J. M. Ballantyne, Solid State Commun. **46**, 95 (1983).
18) D. Heitmann, N. Kroo, C. Schulz, and Z. Szentirmay, Phys. Rev. B **35**, 2660 (1987).
19) Z. Sun and X. Zuo, Opt. Lett. **34**, 1411 (2009).